Published in final edited form as:
Genesis. 2009 October ; 47(10): 680–687. doi:10.1002/dvg.20547.

Generation of conditional *Hoxc8* loss-of-function and *Hoxc8->Hoxc9* replacement alleles in mice

Jessica Blackburn[1,2], **Melissa Rich**[1,3], **Nima Ghitani**[1,4], and **Jeh-Ping Liu**[1]
[1]Department of Neuroscience, University of Virginia School of Medicine, Charlottesville, VA

Abstract

The Hox family of transcription factors are expressed at different domains along the rostrocaudal (R-C) body axis during development. To examine the function of *Hoxc8* and *Hoxc9* in specific cell types and at different developmental times, we have generated and characterized *loxP* flanked (floxed) *Hoxc8* and *Hoxc8->Hoxc9* replacement alleles of mice, with either GFP or LacZ reporters. Although all four alleles of mice behave like wild-type controls in motor behavioral testing, slight differences in endogenous *Hox* gene expression were observed among these alleles depending on the type of reporters used and the presence of *Hoxc9* cDNA in the targeting constructs. The efficiency of Cre-mediated recombination was evaluated by crossing these mice with the *Nestin-cre* and *Isl1-cre* mice, and the loss of Hoxc8 expression with or without Hoxc9 misexpression was confirmed in embryonic spinal cord. In addition, an up-regulation of reporter gene expression was observed after Cre-mediated recombination. These mice will be useful tools to analyze *Hox* gene function in a cell type-specific manner.

Homeotic/Hox genes play important roles in defining cellular identity along the rostrocaudal (R-C) body axis during development (Krumlauf, 1994). The function of *Hox* genes in determining neuronal identity in the hindbrain has been well studied (Keynes and Krumlauf, 1994), while much less is known about their roles in spinal cord development. The expression domains of various *Hox-c* genes have been shown to correlate with the positions of motor neuron (MN) columns and pools (Dasen *et al.*, 2003; Dasen *et al.*, 2005; Liu *et al.*, 2001). In addition, both gain- and loss-of-function experiments performed in chick embryos demonstrate that *Hox6* and *Hox9* paralog groups play instructive roles in defining MN columnar identity, while the *Hox4*, *Hox5*, *Hox7*, and *Hoxc8* groups of genes delineate different motor pools (Dasen *et al.*, 2003; Dasen *et al.*, 2005). Mouse mutants that have lost *Hox9* and *Hox10* function exhibit locomotion deficits in the hindlimb region (Carpenter *et al.*, 1997; de la Cruz *et al.*, 1999; Lin and Carpenter, 2003; Wu *et al.*, 2008), while loss of *Hoxc8* function results in a forelimb prehension-deficiency phenotype (Tiret *et al.*, 1998).

Hox genes are expressed in multiple tissues during development and their expression patterns change with time, and therefore, the motor behavior deficits observed in *Hox* mutants could be a compound effect of losing *Hox* function in both neural and mesodermal tissues. Moreover, neural expression of *Hox* genes is not limited to MNs, as many spinal interneurons required for coordinated locomotion also express various *Hox* genes. Thus, cell type-specific analyses will be required to further decipher the role of *Hox* genes in spinal cord development. To generate conditional loss-of-function and gain-of-function alleles of

Correspondence should be addressed to: Jeh-Ping Liu, Department of Neuroscience, University of Virginia, 409 Lane Road, MR4, Rm. 5032, Charlottesville, VA 22908, Tel: 434-924-8647, Fax: 434-982-4380, jl7nf@virginia.edu.
[2]Current address: Department of Biochemistry, Dartmouth Medical School, Hanover, NH
[3]Current address: MD Program, Virginia Commonwealth University School of Medicine, Richmond, VA
[4]Current address: Neuroscience Training Program, University of Wisconsin, Madison, WI

Hox genes in mouse, we first focused on the *Hoxc8* locus, and used the forelimb grip-deficiency phenotype as a landmark to evaluate floxed *Hoxc8* and *Hoxc8->c9* alleles of mice.

To generate the floxed *Hoxc8* allele, a *loxP* site was inserted in the 5′non-coding region of the *Hoxc8* gene, and a second *loxP* site in the same orientation was inserted 3′ to the three known *Hoxc8* polyadenylation (pA) signals. The endogenous 5′splicing donor site (5′SD), intron 1, and the endogenous 3′ splicing acceptor site (3′SA) were also inserted downstream of the second *loxP* site. We preserved the endogenous intron not only because it contains essential regulatory elements (Awgulewitsch *et al.*, 1990), but also because it has the potential to stabilize the primary, and spliced transcript (Huang and Gorman, 1990). A ribosome reentry site (IRES) followed by either an eGFP (Mombaerts *et al.*, 1996, for tracing axons) or nlsLacZ (nuclear localized LacZ, for marking nuclei) reporter cassette was inserted 3′ to the 3′SA to be used as tracers for the Cre-mediated recombination event. The endogenous 3′ untranslated region (3′UTR) was added 3′ to the reporter sequences. The 3′UTR is included to conserve potential miRNA binding sites that regulate the expression of Hoxc8 (Yekta *et al.*, 2004). A neomycin phosphotransferase (Neo) resistance cassette was also included for positive selection of the transfected ES cells (Fig. 1a).

We also generated conditional *Hoxc8->Hoxc9* replacement alleles to examine the long-term effects of *Hoxc9* misexpression in mouse. To generate the *floxed Hoxc8->c9 allele*, a DNA fragment containing the *Hoxc9* coding region was inserted between the second *loxP* site and the additional *Hoxc8* intron (Fig. 1a). Two floxed *Hoxc8* alleles—one with a GFP reporter, the other with a LacZ reporter, and two floxed *Hoxc8->Hoxc9* alleles, with either GFP or LacZ reporters were generated using this strategy.

Since the *Hox* locus is tightly regulated, any alteration at this locus could potentially affect the expression of surrounding genes. We therefore, characterized these floxed alleles prior to Cre-mediated recombination to ascertain that they behave similar to the wild-type (WT) alleles. We first examined *Hoxc6-Hoxc9* mRNA expression in e10.5 mouse embryos using whole-mount *in situ* hybridization. The expression domains of *Hoxc6* and *Hoxc9* are very similar among embryos carrying different floxed alleles and their WT littermates at e10.5 (data not shown). However, a ~1-segment rostral extension in neural and mesodermal *Hoxc8* expression domain was observed in the GFP-tagged *Hoxc8->c9*$^{F/F}$ (*Hoxc8->c9*$^{F/F}$*-GFP*) embryos (Fig. 2c), while a ~2-segment rostral extension in the neural and a ~3-segment rostral extension in the mesodermal *Hoxc8* expression domains were observed in the LacZ-tagged *Hoxc8*$^{F/F}$ (*Hoxc8*$^{F/F}$*-LacZ*) and *Hoxc8->c9*$^{F/F}$ (*Hoxc8->c9*$^{F/F}$*-LacZ*) embryos (Fig. 2d, e). The GFP-tagged *Hoxc8*$^{F/F}$ (*Hoxc8*$^{F/F}$*-GFP*) embryos exhibit no apparent change in *Hoxc8* expression domain as compared to the WT controls (Fig. 2a, b).

To examine the phenotypic consequences of these changes in mesodermal tissues, we performed skeletal staining in e18.5 mouse embryos from different alleles prior to Cre-mediated recombination. WT and the *Hoxc8*$^{F/F}$*-GFP* embryos have 7 cervical vertebrae (C1–C7) and their 6th and 7th ribs (R6s and R7s) are attached to the sterna (Fig. 2f, g, k, l). However, extra ribs extending from the C7 and elongated R8s attached to the sterna were observed in *Hoxc8*$^{F/F}$*-LacZ* and *Hoxc8->c9*$^{F/F}$*-LacZ* embryos (Fig. 2i, j, n, o). The F/+ embryos derived from these two LacZ-tagged alleles have a milder phenotype with either a partial rib extending from the C7 or only one of the R8s attached to the sternum (data not shown). The majority of the *Hoxc8->c9*$^{F/F}$*-GFP* embryos have normal C7vertebra, but their R8s are attached to the sterna (Fig. 2m). No obvious homeotic transformation in skeletons was observed in the *Hoxc8->c9*$^{F/+}$*-GFP* embryos (data not shown).

To ascertain that the minor changes observed in the *Hoxc8* expression domain did not impair motor function, we examined 2-month old male mice for their forelimb grip strength, a phenotype that was observed in the *Hoxc8*$^{-/-}$ animals previously (Tiret *et al.*, 1998). We found no deficit in the grip strength in all 4 floxed alleles of mice when compared to their WT littermates (Fig. 2p), indicating that the minor change observed in the *Hoxc8* expression domain did not cause impairment of motor function.

Because of our interest in *Hox* gene function during spinal cord development, we further evaluated the endogenous *Hox* gene expression in open-book spinal cord preparations from e13.5 embryos by whole mount *in situ* hybridization prior to Cre-mediated recombination. We focused our examination on the GFP-tagged floxed alleles that exhibit little or no deviation in endogenous *Hox* gene expression from the WT allele. The R-C levels were estimated from the positions of the dorsal root ganglia (DRG) that remain attached to the spinal cord during this procedure (see Methods). Slight changes in the *Hoxc8* mRNA rostral expression boundary were observed in *Hoxc8*$^{F/F}$*-GFP*, *Hoxc8->c9*$^{F/+}$*-GFP*, and *Hoxc8->c9*$^{F/F}$*-GFP* embryos when compared to WT controls (Fig. 3a, c–e), including a caudal shift of expression at the intermediate region and a more uniform expression in the ventral region of the spinal cord. No obvious change in *Hoxc8* mRNA expression was detected in the *Hoxc8*$^{F/+}$*-GFP* embryos (Fig. 3b). No significant change in *Hoxc6* mRNA expression was observed between various floxed alleles and WT controls (data not shown). In contrast, the rostral boundary of *Hoxc9* mRNA expression in the *Hoxc8->c9*$^{F/F}$*-GFP* ventral spinal cord is shifted ~ 1 segment caudally when compared to WT controls (Fig. 3f, j), while no significant change in *Hoxc9* mRNA expression was detected in *Hoxc8*$^{F/+}$*-GFP*, *Hoxc8*$^{F/F}$*-GFP*, and *Hoxc8->c9*$^{F/+}$*-GFP* embryos (Fig. 3g–i).

Hoxc6 protein induces lateral motor column (LMC) formation in the brachial level spinal cord while Hoxc9 protein induces the formation of sympathetic preganglionic neurons in the thoracic level spinal cord. Cross-inhibitory actions between these two proteins at the junction between brachial and thoracic levels delineate the brachial vs. thoracic identity of individual cells (Dasen *et al.*, 2003). We therefore examined the mRNA expression of an LMC marker, *Raldh2*, which is induced by Hoxc6 and suppressed by Hoxc9 proteins. The *Raldh2* expression domain extends caudally by ~1 segment in the *Hoxc8->c9*$^{F/F}$*-GFP* embryos compared to the WT (Fig. 3k, o), and this could result from the caudally displaced *Hoxc9* rostral expression boundary. No significant change in *Raldh2* mRNA expression was observed in *Hoxc8*$^{F/+}$*-GFP*, *Hoxc8*$^{F/F}$*-GFP*, and *Hoxc8->c9*$^{F/+}$*-GFP* spinal cords compared to the WT controls (Fig. 3l–n).

Hoxc8 protein defines motor pool identity in the caudal cervical level spinal cord, and we therefore examined the mRNA expression of a motor pool marker, *Pea3*, that is a downstream target of Hoxc8 (Vermot *et al.*, 2005). We did not observe significant differences in the *Pea3* expression domains in *Hoxc8*$^{F/+}$*-GFP*, *Hoxc8*$^{F/F}$*-GFP*, and *Hoxc8->c9*$^{F/+}$*-GFP* embryos compared to the controls (Fig. 3p–s). However, in the *Hoxc8->c9*$^{F/F}$*-GFP* embryos, the *Pea3* expression domain is extended caudally (~1 segment, Fig. 3t), and this could be a secondary effect of the caudally expanded *Raldh2* expression domain which also extended the caudal motor pools (Fig. 3o). These results further demonstrate the sensitivity of the *Hoxc* locus to genomic manipulation—although these four targeting constructs share the same basic design, subtle changes in endogenous *Hox* gene expression could occur depending on the type of reporters used, and the presence of the *Hoxc9* cDNA in individual targeting constructs. Although we are not certain which component of the exogenous DNA caused this difference, the size difference between the GFP and LacZ reporters (~0.8kb vs. ~3kb) and the presence of an additional ~0.8 kb *Hoxc9* cDNA sequence could be one of the possibilities.

To determine if *Hoxc8* expression can be eliminated or replaced by *Hoxc9* expression after Cre-mediated recombination, we crossed the floxed *Hoxc8-GFP* and *Hoxc8->c9-GFP* mice with *Nestin-cre* (*Nescre*) (Tronche *et al.*, 1999), and *Isl1-cre* (*Isl1cre*) (Srinivas *et al.*, 2001) transgenic mice, and examined Hox protein expression using immunohistochemistry on cross-sectioned spinal cord tissue obtained from e12.5 mouse embryos. By e12.5, the majority of cells in the spinal cord of the *Hoxc8*$^{F/F}$*-GFP;Nescre* and *Hoxc8->c9*$^{F/F}$*-GFP;Nescre* embryos had already lost Hoxc8 protein expression (Fig. 4d, f, and data not shown). In the *Hoxc8->c9*$^{F/F}$*-GFP; Nescre* embryos, ectopic Hoxc9 protein expression at the expense of endogenous Hoxc8 protein is clearly visible using antibodies against either Hoxc8 or Hoxc9 (Fig. 4d, e). However, the Hoxc9 protein expression is not as high as that of the endogenous Hoxc8 protein but instead, is more similar to the endogenous Hoxc9 expression observed at the thoracic levels (Fig. 4a, d, and data not shown), this could reflect a difference in the properties between the anti-Hoxc8 and anti-Hoxc9 antibodies used, or a brachial to thoracic fate change induced by Hoxc9 misexpression. A reduction of Hoxc6 protein expression in these cells is also apparent when compared to the controls (Fig. 4b, c, e, f), demonstrating that misexpression of Hoxc9 reduces the expression of endogenous Hoxc6. Essentially none of the Isl1^{+} neurons co-express Hoxc8 in e12.5 *Hoxc8*$^{F/F}$*-GFP;Isl1cre* and *Hoxc8->c9*$^{F/F}$*-GFP;Isl1cre* embryos, even in the lateral LMC (LMCl) MNs where Isl1 is only expressed transiently (Fig 4g, h, and data not shown), suggesting that the *Isl1-cre* has a higher recombination efficiency than *Nestin-cre*. A higher level of GFP expression can be activated in embryos that have undergone the Cre-mediated recombination and can be observed in freshly dissected embryos under a fluorescent stereomicroscope in comparison to the low levels of GFP expression observed prior to the recombination. Unfortunately, fixation with paraformaldehyde diminishes the GFP signal and an anti-GFP antibody is required to visualize GFP expression in cross-sectioned spinal cord tissues (Fig. 4i, and data not shown). Similarly, high levels of β-galactosidase activity can be observed in the spinal cord of e11.5 *Hoxc8*$^{F/F}$*-LacZ;Isl1cre* and *Hoxc8->c9*$^{F/F}$*-LacZ;Isl1cre* embryos (Fig. 4k and data not shown) in contrast to the low-level β-galactosidase activity observed prior to Cre-mediated recombination (Fig. 4j). The presence of low-level reporter gene expression prior to Cre-mediated recombination indicates that a small percentage of *Hoxc8* transcripts are not ployadenylated by the 3 known pA signals.

In summary, we have generated conditional *Hoxc8* loss-of-function and *Hoxc8 ->Hoxc9* replacement alleles of mice with either GFP or LacZ reporters. Although all four alleles are indistinguishable from WT controls in motor behavioral testing, molecular analyses revealed that the floxed *Hoxc8-GFP* allele behaved most like the WT in the endogenous *Hox* gene expression. The floxed *Hoxc8->Hoxc9-GFP* allele displayed a ~1 segment rostral expansion of *Hoxc8* mRNA expression at e10.5, and a ~1 segment caudal displacement of the *Hoxc9* mRNA rostral expression boundary in e13.5 spinal cord, while the floxed *Hoxc8-LacZ* and floxed *Hoxc8->Hoxc9-LacZ* alleles exhibited a ~2-segment rostral extension in the neural and a ~3-segment rostral extension in the mesodermal *Hoxc8* mRNA expression domains at e10.5. Upon Cre-mediated recombination, deletion of *Hoxc8* and misexpression of *Hoxc9* along with up-regulated GFP or LacZ expression were observed, demonstrating that these alleles of mice will be useful tools to study *Hox* function in a cell type-specific manner.

Methods

Targeting constructs

To generate *Hoxc8* conditional targeting constructs, a 65bp fragment containing the *LoxP* sequence was cloned into a SacII site within exon1, 5′ to the translation start site. The following sequences were inserted into the Ear1 site (3′ to the 3 known polyadenylation sites) of the *Hoxc8* locus in tandem: a second *LoxP* site in the same orientation followed by a ~1.4kb Nco1-Sal1 fragment containing the *Hoxc8* intron, an IRES-eGFP or an IRES-

nlsLacZ fragment followed by a ~1.5kb BseR1 fragment containing the 3' UTR of *Hoxc8* and the polyadenylation sequence from bovine albumin gene, and a pGKneo cassette for positive selection. The final targeting constructs were assembled in the pMoluc vector (Feng *et al.*, 2002) and contain a ~9.5kb Sph1-Xba1 *Hoxc8* genomic region with the above modifications. The homologus sequence at the 5´ and the 3´ arms are ~2.5kb and ~3.4kb respectively. To generate *Hoxc8->Hoxc9* conditional replacement targeting constructs, a ~0.8kb fragment containing *Hoxc9* coding region was inserted between the 3´*LoxP* site and the 1.4 kb *Hoxc8* intron sequence in the *Hoxc8* conditional knock-out constructs. Targeting constructs were digrested with Not1 and electroporated into W9.5 ES cells as described (Dragatsis *et al.*, 2000). The targeting frequency is ~3%–4% (3 or 4 targeted clones from 96 G418-resistent colonies picked for each construct).

ES cell injection and mouse genotyping

ES cells carrying the targeted alleles were verified by Southern analyses (see below) and were injected into C57BL6 blastocysts using standard procedures (Bradley, 1987). Male chimeras were crossed with C57B/6J females to generate heterozygous offspring. Mice carrying floxed alleles are maintained in a mixed 129/Sv and C57BL6 background and are housed in a barrier facility under 12-hr light/ 12-hr dark cycle. All protocols for animal use were approved by the Institutional Animal Care and Use Committee of the University of Virginia and were in accordance with NIH guidelines.

Genotyping was first performed by Southern blot analysis using Xba1-digested genomic DNA probed with a 500bp 5´-flanking HindIII-Sph1 fragment. PCR genotyping was performed with following primer pairs: LoxP1: 5'-CGCTCTACCTA CG CAGTGAG-3', and LoxP3: 5'-GGAAAACAGGGGGTTGACGAA G-3' (for floxed *Hoxc8*, and floxed *Hoxc8->c9* alleles), LoxP1 and mHoxc8I: 5'-GGAGCGCGGGAGACCAAG-3' (for Δfloxed *Hoxc8* alleles), LoxP1 and Hoxc95R: 5'-CCTGGACGCTAGGAGGTC-3' (for Δfloxed *Hoxc8->c9* alleles).

In situ hybridization, β-galactosidase activity, immunohistochemistry, and skeletal staining

For whole mount in situ hybridization, mouse embryos were harvested at e10.5 (noon of the day that the vaginal plug was present is considered e0.5), and spinal cords were isolated from e13.5 embryos. Dorsal root ganglia (DRG) were left on the dissected spinal cord through the *in situ* hybridization procedure, and images were taken with a Nikon SMZ1500 stereoscope before and after DRG removal to estimate the R-C extent of gene expression. *Raldh2*, *Pea3*, *Sox5*, and *Hoxc6* probes were provided by Drs. T. Jessell and J. Dasen. *Hoxc8* and *Hoxc9* probes were provided by Dr. P. Gruss.

For β-galactosidase staining, e11.5 mouse embryos were fixed for 20' in 4% paraformaldehye in 0.1M PB (phosphate buffer, pH 7.4), then washed 2×15' with Buffer A (5mM EGTA, 2mM $MgCl_2$ in 0.1M PB), and 2×15' with Buffer B (0.2% NP40, 0.1% Sodium Desoxycholate, 2mM $MgCl_2$ in 0.1M PB). Color reaction was performed in Buffer C (0.6mg/ml X-Gal, 5mM $K_3Fe(CN_6)$, 5mM $K_4Fe(CN_6)$, in Buffer B) at 37°C in dark and images were taken using a Nikon SMZ1500 stereoscope.

Immunohistochemistry was performed on 10 μm sections from e12.5 embryos using the following antibodies as described (Liu, 2006): rabbit anti-GFP (Invitrogen), mouse anti-Hoxc8 (Covance), rabbit and guinea pig anti-Isl1 (provided by Dr. T. Jessell), guinea pig anti-Hoxc6, and rabbit anti-Hoxc9 (Liu *et al.*, 2001). Images were taken with a Nikon C1 confocal microscope.

Mouse embryos were harvested at e18.5 and processed for skeleton staining as described (McLeod, 1980).

Grip strength testing

Forelimb grip strength testing was performed with three trials using a grip strength apparatus (San Diego Instruments, Inc.). Graphs and statistical analyses were generated using SigmaPlot.

References

Awgulewitsch A, Bieberich C, Bogarad L, Shashikant C, Ruddle FH. Structural analysis of the Hox-3.1 transcription unit and the Hox-3.2-- Hox-3.1 intergenic region. Proc Natl Acad Sci U S A. 1990; 87:6428–6432. [PubMed: 1696731]

Bradley, A. Production and analysis of chimeric mice. In: Robertson, EJ., editor. Teratocarcinomas and Embryonic Stem Cells: A Practical Approach. Oxford: IRL Press; 1987. p. 131-151.

Carpenter EM, Goddard JM, Davis AP, Nguyen TP, Capecchi MR. Targeted disruption of Hoxd-10 affects mouse hindlimb development. Development. 1997; 124:4505–4514. [PubMed: 9409668]

Dasen JS, Liu JP, Jessell TM. Motor neuron columnar fate imposed by sequential phases of Hox-c activity. Nature. 2003; 425:926–933. [PubMed: 14586461]

Dasen JS, Tice BC, Brenner-Morton S, Jessell TM. A Hox regulatory network establishes motor neuron pool identity and target-muscle connectivity. Cell. 2005; 123:477–491. [PubMed: 16269338]

de la Cruz CC, Der-Avakian A, Spyropoulos DD, Tieu DD, Carpenter EM. Targeted disruption of Hoxd9 and Hoxd10 alters locomotor behavior, vertebral identity, and peripheral nervous system development. Dev Biol. 1999; 216:595–610. [PubMed: 10642795]

Dragatsis I, Levine MS, Zeitlin S. Inactivation of Hdh in the brain and testis results in progressive neurodegeneration and sterility in mice. Nat Genet. 2000; 26:300–306. [PubMed: 11062468]

Feng T, Li Z, Jiang W, Breyer B, Zhou L, Cheng H, Haydon RC, Ishikawa A, Joudeh MA, He TC. Increased efficiency of cloning large DNA fragments using a lower copy number plasmid. Biotechniques. 2002; 32:992. [PubMed: 12019795]

Huang MT, Gorman CM. Intervening sequences increase efficiency of RNA 3' processing and accumulation of cytoplasmic RNA. Nucleic Acids Res. 1990; 18:937–947. [PubMed: 1690394]

Keynes R, Krumlauf R. Hox genes and regionalization of the nervous system. Annual Review of Neuroscience. 1994; 17:109–132.

Krumlauf R. Hox genes in vertebrate development. Cell. 1994; 78:191–201. [PubMed: 7913880]

Lin AW, Carpenter EM. Hoxa10 and Hoxd10 coordinately regulate lumbar motor neuron patterning. J Neurobiol. 2003; 56:328–337. [PubMed: 12918017]

Liu JP. The function of growth/differentiation factor 11 (Gdf11) in rostrocaudal patterning of the developing spinal cord. Development. 2006; 133:2865–2874. [PubMed: 16790475]

Liu JP, Laufer E, Jessell TM. Assigning the Positional Identity of Spinal Motor Neurons. Rostrocaudal Patterning of Hox-c Expression by FGFs, Gdf11, and Retinoids. Neuron. 2001; 32:997–1012. [PubMed: 11754833]

McLeod MJ. Differential staining of cartilage and bone in whole mouse fetuses by alcian blue and alizarin red S. Teratology. 1980; 22:299–301. [PubMed: 6165088]

Mombaerts P, Wang F, Dulac C, Chao SK, Nemes A, Mendelsohn M, Edmondson J, Axel R. Visualizing an olfactory sensory map. Cell. 1996; 87:675–686. [PubMed: 8929536]

Srinivas S, Watanabe T, Lin CS, William CM, Tanabe Y, Jessell TM, Costantini F. Cre reporter strains produced by targeted insertion of EYFP and ECFP into the ROSA26 locus. BMC Dev Biol. 2001; 1:4. [PubMed: 11299042]

Tiret L, Le Mouellic H, Maury M, Brulet P. Increased apoptosis of motoneurons and altered somatotopic maps in the brachial spinal cord of Hoxc-8-deficient mice. Development. 1998; 125:279–291. [PubMed: 9486801]

Tronche F, Kellendonk C, Kretz O, Gass P, Anlag K, Orban PC, Bock R, Klein R, Schutz G. Disruption of the glucocorticoid receptor gene in the nervous system results in reduced anxiety. Nat Genet. 1999; 23:99–103. [PubMed: 10471508]

Vermot J, Schuhbaur B, Le Mouellic H, McCaffery P, Garnier JM, Hentsch D, Brulet P, Niederreither K, Chambon P, Dolle P, Le Roux I. Retinaldehyde dehydrogenase 2 and Hoxc8 are required in the murine brachial spinal cord for the specification of Lim1+ motoneurons and the correct distribution of Islet1+ motoneurons. Development. 2005; 132:1611–1621. [PubMed: 15753214]

Wu Y, Wang G, Scott SA, Capecchi MR. Hoxc10 and Hoxd10 regulate mouse columnar, divisional and motor pool identity of lumbar motoneurons. Development. 2008; 135:171–182. [PubMed: 18065432]

Yekta S, Shih IH, Bartel DP. MicroRNA-directed cleavage of HOXB8 mRNA. Science. 2004; 304:594–596. [PubMed: 15105502]

Acknowledgments

We thank S. Zeitlin for discussion and comments on this manuscript; T.-C. He for providing the pMOLUC vector. This work was supported by NIH grant NS045933 to J.-P. Liu.

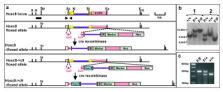

Figure 1. Generation of *Hoxc8* conditional loss-of-function and *Hoxc8* replaced by *Hoxc9* mouse alleles

(a) *Hoxc8* genomic locus. E1 and E2 represent Exon1 and 2, yellow boxes represent coding region, purple lines represent the intron, and pink boxes represent the 3´ untranslated region (UTR). X=Xba1, H=HindIII, Sp=Sph1, Sc=SacII, N=Nco1, Sl=Sal1, Ea=Ear1. Targeting constructs contain ~9.5kb genomic DNA from the 5´ Sph1 site to the 3´ Xba1 site. “IR” represents internal ribosome reentry site, “marker” represents either eGFP or nlsLacZ reporter used in various versions of the targeting constructs. A Black box indicates the HindII-Sph1 fragment used as a probe for the Southern blot shown in (b). Black triangles indicate the positions of LoxP1 and LoxP3 primers used in (c).

(b) Southern analyses. Genomic DNA digested with Xba1 and probed with a 500bp HindIII-Sph1 probe identified a ~10.4kb wild-type (+) band. For the *Hoxc8-LacZ* allele, the size of the targeted band (F) is ~19.2kb (group 1). For the *Hoxc8-GFP*, *Hoxc8->c9-GFP*, and *Hoxc8->c9-LacZ* alleles, the size of the targeted band (F) is ~7kb (group 2).

(c) PCR reactions using LoxP1 and LoxP3 primers. The wild-type allele (+) produces a ~230bp band while the targeted allele (F) produces a ~300bp band.

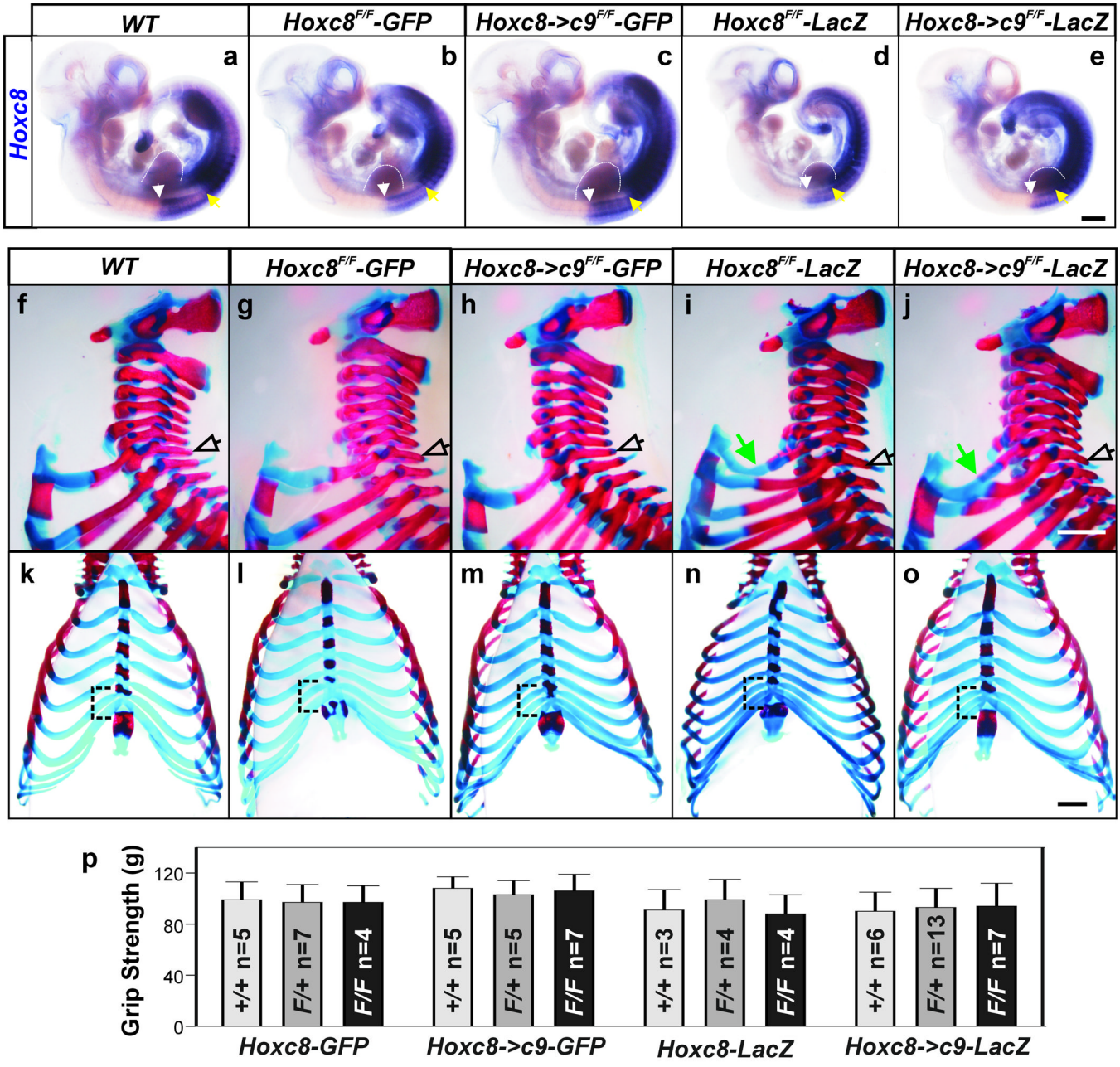

Figure 2. Phenotypic evaluation of floxed *Hoxc8* and floxed Hoxc8->c9 alleles prior to Cre-mediated recombination

(a–e) *Hoxc8* mRNA expression in e10.5 embryos revealed by whole mourn*t in situ* hybridization, dashed lines mark the position of the forelimbs.

In wild-type (a) and *Hoxc8$^{F/F}$- GFP* (b) embryos, the rostral boundary of *Hoxc8* expression in the ventral neural tube is located at ~s8 (white arrows), while the rostral boundary of mesodermal expression is located ~s13 (yellow arrows). In a *Hoxc8->c9$^{F/F}$- GFP* embryo (c), the rostral boundary of neural *Hoxc8* expression is located at ~s7 (white arrow), while the rostral boundary of mesodermal expression is located ~s12 (yellow arrow). In *Hoxc8$^{F/F}$- LacZ* (d) and *Hoxc8->c9$^{F/F}$- LacZ* (e) embryos, the rostral boundary of neural *Hoxc8* expression is located at ~s6 (white arrows), while the rostral boundary of mesodermal expression is located ~ s10 (yellow arrows). Scale bar=0.5mm.

(f–j) Lateral view of vertebral columns at cervical to rostral thoracic levels from e18.5 embryos. Cartilage is stained by Alcian Blue BGX and ossified bones are stained by Alizarin Red S. Wild-type (f), *Hoxc8*$^{F/F}$*- GFP* (g), and *Hoxc8->c9*$^{F/F}$*- GFP* (h) embryos have 7 cervical vertebrae with their first rib originating from the first thoracic vertebra (open arrows), while *Hoxc8*$^{F/F}$*- LacZ* (i), and *Hoxc8->c9*$^{F/F}$*- LacZ* (j) embryos exhibit an anterior transformation with an extra rib originating from C7 (green arrows).
(k–o) Ventral view of the rib cages from e18.5 embryos. In wild-type (k) and *Hxoc8*$^{F/F}$*-GFP* (l) embryos, the 6th and the 7th ribs are the last two ribs attached to the sterna (black brackets). In *Hoxc8->c9*$^{F/F}$*- GFP* (m), as well as *Hoxc8*$^{F/F}$*- LacZ* (n) and *Hoxc8->c9*$^{F/F}$*-LacZ* (o) embryos, their 8th ribs are also attached to the sterna (black brackets). Scale bars=1mm.
(p) Forelimb grip strength of *Hoxc8*$^{F/+}$, *Hoxc8*$^{F/F}$, *Hoxc8->c9*$^{F/+}$, and *Hoxc8->c9*$^{F/F}$ adult male mice with either GFP or LacZ reporters, compared to their wild-type littermates. No significant difference was observed between different genotypes within each allele.

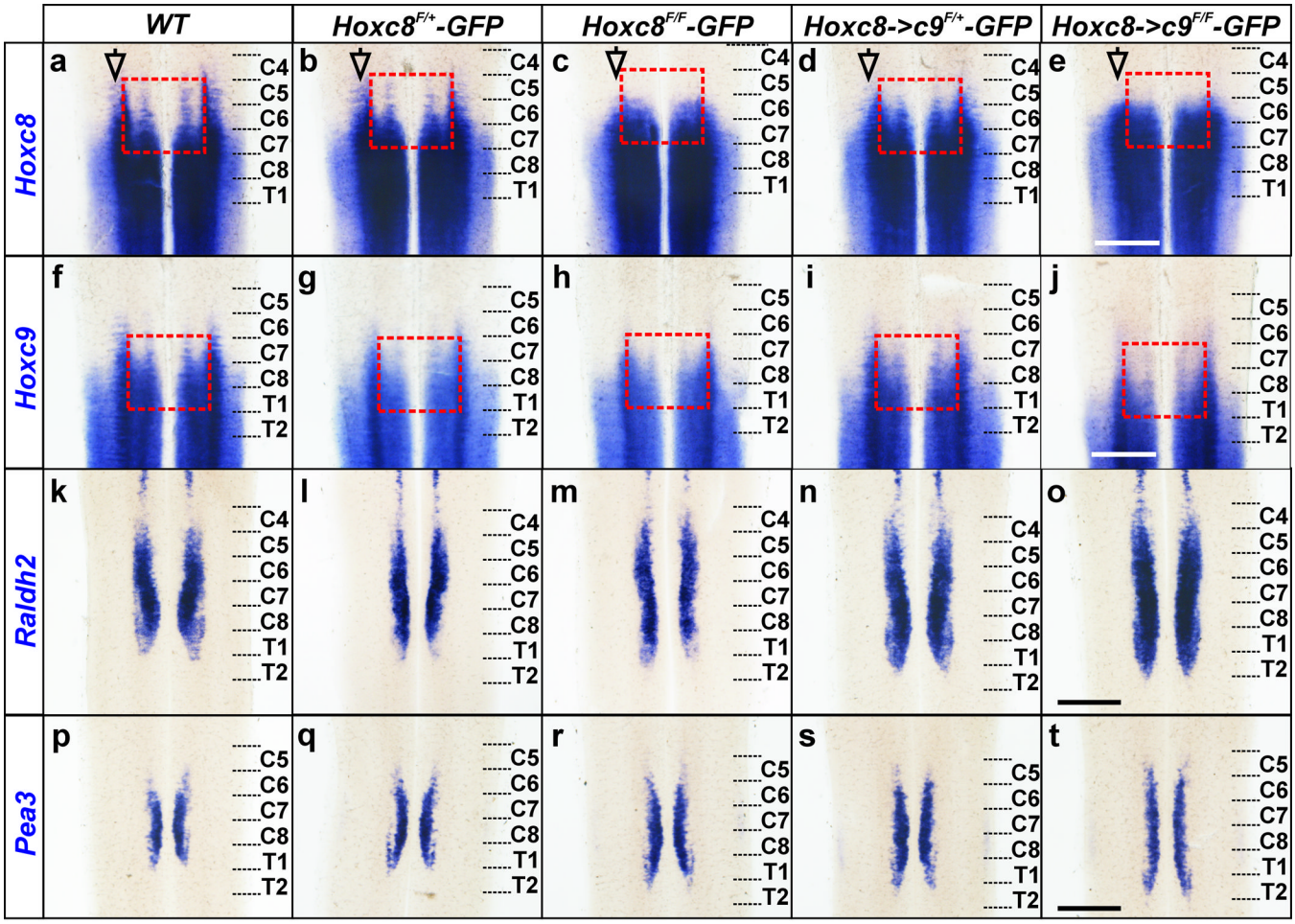

Figure 3. Marker analyses in e13.5 embryonic spinal cords derived from GFP-tagged floxed *Hoxc8* and floxed *Hoxc8->c9* alleles prior to Cre-mediated recombination

(a–e) *Hoxc8* mRNA expression in open-book preparations of e13.5 embryonic spinal cords. Slight changes in the rostral boundary of *Hoxc8* expression domain in the ventral (red boxed areas) and intermediate (open arrows) spinal cord are observed in *Hoxc8*$^{F/F}$*-GFP* (c), *Hoxc8->c9*$^{F/+}$*-GFP* (d), and *Hoxc8->c9*$^{F/F}$ *-GFP* (e) embryos as compared to the wild-type (a) and *Hoxc8*$^{F/+}$ *-GFP* (b) embryos.

(f–j) *Hoxc9* mRNA expression in open-book preparations of e13.5 embryonic spinal cords. *Hoxc9* rostral expression boundary (red boxed area) in the *Hoxc8->c9*$^{F/F}$ *-GFP* (j) embryos is placed ~1 segment caudally when compared to the rest of embryos (f–i).

(k–o) mRNA expression of an LMC marker, *Raldh2*, in open-book preparations of e13.5 embryonic spinal cords. ~1 segment caudal extension of *Raldh2* expression is observed in the *Hoxc8->c9*$^{F/F}$ *-GFP* embryo (o) compared to the rest of embryos (k–n).

(p–t) mRNA expression of a motor pool marker, *Pea3*, in open-book preparations of e13.5 embryonic spinal cords. A caudal expansion of *Pea3* expression is observed in *Hoxc8->c9*$^{F/F}$*-GFP* embryos (t). Scale Bars=0.5mm.

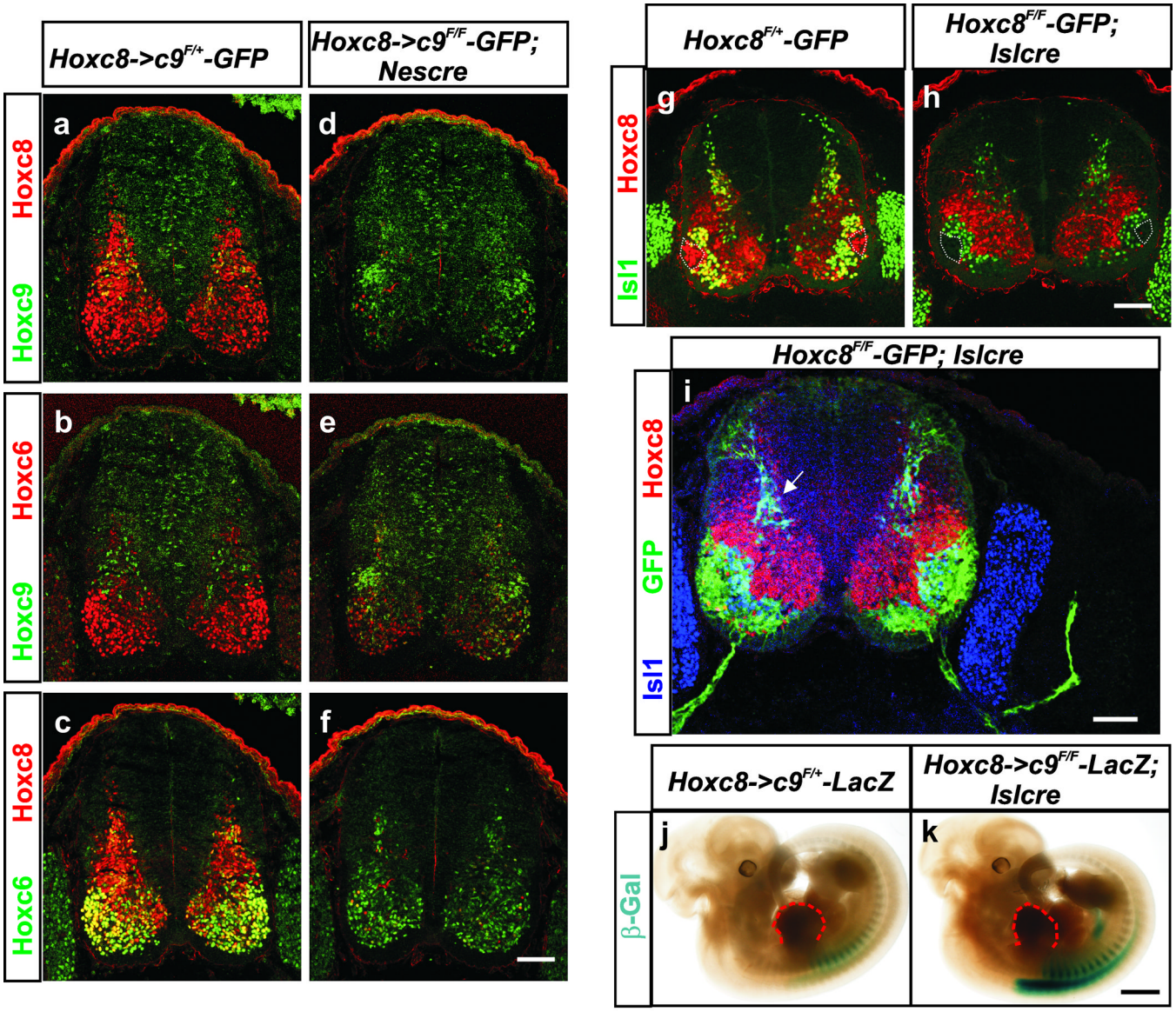

Figure 4. Changes in Hox and reporter protein expression after Cre-mediated recombination

(a–f) Immunohistochemistry using anti-Hoxc6, anti-Hoxc8, and anti-Hoxc9 antibodies in cross-sectioned e12.5 caudal cervical level spinal cord. Many Hoxc6^{+} and Hoxc8^{+}, but few Hoxc9^{+} cells are present in *Hoxc8->c9$^{F/+}$-GFP* embryos (a–c). Several remaining Hoxc8^{+} cells along with increased Hoxc9 and decreased Hoxc6 expression are visible in the *Hoxc8->c9$^{F/F}$-GFP; Nescre* spinal cord (d–f).

(g–h) Immunohistochemistry using anti-Hoxc8 and anti-Isl1 antibodies in cross-sectioned caudal cervical level e12.5 spinal cord. There is no overlap between Isl1 and Hoxc8 expression in a *Hoxc8$^{F/F}$-GFP;Islcre* (h) embryo compared to the control littermate (g). Hoxc8 expression is also absent in LMCl MNs (marked by white dashed lines) where Isl1 is only expressed transiently (h).

(i) Cross-sectioned spinal cord from an e12.5 *Hoxc8$^{F/F}$-GFP;Islcre* embryo showing high levels of GFP expression revealed by an anti-GFP antibody in dI3 interneurons (white arrow) and in MNs lacking Hoxc8 expression, while low levels of GFP expression are

observed in Hoxc8^{+} neurons. GFP expression is also visible in the axons. Scale bars=100μm.

(j–k) High levels of β-galactosidase activity are observed in the spinal cord of an e11.5 *Hoxc8->c9$^{F/F}$-LacZ;Islcre* embryo (k) compares to the low-level β-galactosidase activity present in the spinal cord and mesoderm in their *Hoxc8->c9$^{F/+}$* littermates (i). Red dotted lines mark the position of the forelimbs. Scale bar=1 mm.